Antireflection properties and solar cell application of silicon nanoscructures*

Yue Huihui(岳会会), Jia Rui(贾锐)†, Chen Chen(陈晨), Ding Wuchang(丁武昌), Wu Deqi(武德起), and Liu Xinyu(刘新宇)

Key Laboratory of Microwave Devices and Integrated Circuits, Institute of Microelectronics, Chinese Academy of Sciences, Beijing 100029, China

Abstract: Silicon nanowire arrays (SiNWAs) are fabricated on polished pyramids of textured Si using an aqueous chemical etching method. The silicon nanowires themselves or hybrid structures of nanowires and pyramids both show strong anti-reflectance abilities in the wavelength region of 300–1000 nm, and reflectances of 2.52% and less than 8% are achieved, respectively. A 12.45% SiNWAs-textured solar cell (SC) with a short circuit current of 34.82 mA/cm^2 and open circuit voltage (V_{oc}) of 594 mV was fabricated on 125 × 125 mm^2 Si using a conventional process including metal grid printing. It is revealed that passivation is essential for hybrid structure textured SCs, and V_{oc} can be enlarged by 28.6% from 420 V to 560 mV after the passivation layer is deposited. The loss mechanism of SiNWA SC was investigated in detail by systematic comparison of the basic parameters and external quantum efficiency (EQE) of samples with different fabrication processes. It is proved that surface passivation and fabrication of a metal grid are critical for high efficiency SiNWA SC, and the performance of SiNWA SC could be improved when fabricated on a substrate with an initial PN junction.

Key words: antireflection properties; silicon nanowires; solar cells; passivation

DOI: 10.1088/1674-4926/32/8/084005 **PACC:** 7865H; 8630J; 6146 **EEACC:** 2520C; 2550N

1. Introduction

Surface antireflection techniques are important for the performance enhancement of many optical devices, such as SCs and planar displays[1−3]. Conventionally, transparent quarter wavelength layers of SiO_x, TiO_x, or Si_xN_y with intermediate or gradient refractive indices are used as antireflection coatings, although multilayer coatings have also been used to broaden the spectral width of the antireflection. However, these coatings work effectively only in a limited spectral range and for specific angles of incidence[4]. An alternative approach to minimize reflectivity utilizes a fine textured surface, comprising sub-wavelength structural features on the nanometer scale. A sub-wavelength structure surface with a deep and tapered profile can suppress the Fresnel reflection substantially over a wide spectral bandwidth. The fabrication of the sub-wavelength structures haw been investigated by several methods, including chemical vapor deposition[5], laser ablation[6] and annealing in a reactive atmosphere[7−9]. Although these synthesis methods are quite acceptable and well controlled, most need either a high synthesis temperature or a long synthesis time[10] due to the limitation of the growth mechanism, and this increases the production cost. A silver induced aqueous-chemical-etching process conveniently synthesizes SiNWAs at low cost compared to the above methods[10]. However, no analyses have been undertaken on how SiNWAs could be synthesized on pyramid textured Si wafer. Simultaneously, Si NW array SCs have been reported by many institutes, but less work has been done on the loss mechanism from the EQE aspect[10−12].

In this work, SiNWAs synthesized by a galvanic displacement reaction were explored to replace the conventional pyramid textured (CPT) structure for crystal Si (C-Si) SCs. SiNWAs are produced on both polished and CPT Si. It is proved that SiNWA can be conveniently synthesized on the sidewall of the pyramids to form a hybrid structure, which is almost independent of the crystallographic orientation. The SiNWAs prepared on polished Cz-Si show a significantly lower reflectance of 2.53% in the wavelength region of 300–1000 nm. The lowest reflectance of the hybrid structured Si is 8%, which is also much lower than pyramid textured Si. Also, the reflectance property of the SiNWAs versus etching duration is studied in detail. SiNWA SC with an efficiency of 12.45% has been achieved, as the short circuit current is enlarged prominently. The effects of the SiNWAs on the performance of the cell, such as the external quantum efficiency (EQE), the conversion efficiency (η), open circuit voltage (V_{oc}), and short circuit current (I_{sc}), have been systemically investigated.

2. Experiment section

SiNWAs were fabricated on 280 μm p-type double side polished (substrates A) and one side pyramid textured (substrates B) Cz-Si (100) substrates with resistivity of 0.9 Ω·cm. Various lengths of SiNWAs were obtained by immersing Si substrate in aqueous 4.6M hydrofluoric acid (HF) and 0.02M silver nitrate ($AgNO_3$) mixture solution, and soaking the wafer

* Project supported by the State Key Development Program for Basic Research of China (Nos. 2006CB604904, 2009CB939703), the National Natural Science Foundation of China (Nos. 60706023, 90401002, 60977050, 90607022), and the Chinese Academy of Solar Energy Action Plan (No.YZ0635).

† Corresponding author. Email: jiarui@ime.ac.cn

Received 15 February 2011

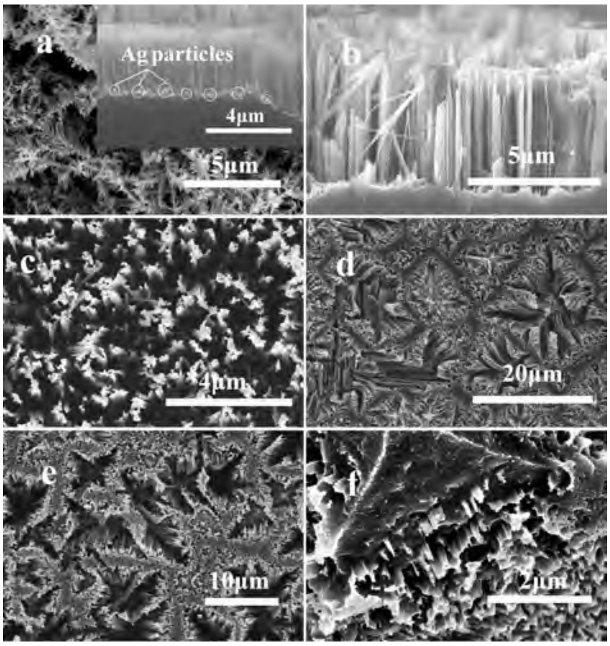

Fig. 1. (a) Silver films on substrate A after etching for 2 h; the inset shows the silver particle at the bottom of the NWs. (b) SEM of the Ag removed NWs on substrate etched for 2 h. (c) Top view of substrate A etched for 3 h. (d), (e) Top view of substrate B etched for 2 and 3 h. (f) Magnified top view of substrate B etched for 0.5 h.

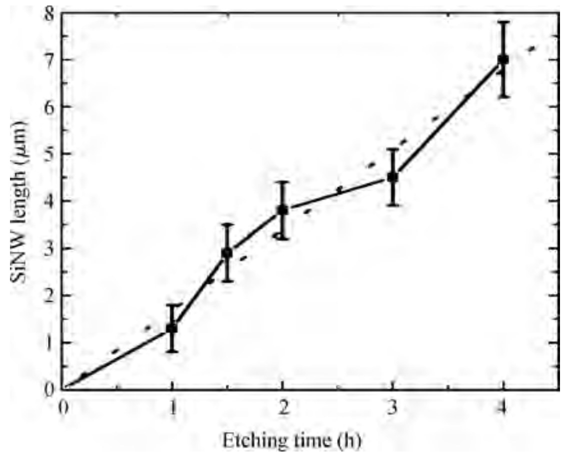

Fig. 2. Relationship of length of SiNWAs versus etching duration. The dotted line is the linear fit relationship.

in a hydrothermal bath of 25 ℃ for times from 30 to 240 min. Increased etching time results in correspondingly longer wire-length l. During the etching process, Ag particles were produced on the silicon surface and catalyzed subsequent Si etching by acting as local cathodes while the Si below Ag acts as anodes. Concentrated nitric acid (HNO_3) etching for 1 h has been applied to remove the residual Ag particle, followed by a rinse in 5% HF solution for 30 s and DI water three times to eliminate the oxide layer and residual ion, respectively. The Ag mass concentration ratio falls below 0.5% in 10 μm^2 areas at the bottom position of SiNWAs by energy diffuse spectrometry analysis. Reflectance and transmittance of various-length SiNWAs were measured on a 7-SCSpec SC spectral measurements system.

SCs were fabricated on SiNWAs textured substrates, hybrid structure of SiNWAs and pyramid structure textured substrates and C-Si substrates with PN junctions. Conventional silicon cell fabrication processes were used to form a front phosphorous-diffused emitter, Al back-surface field as well as metal grid. The basic parameters including η, I_{sc}, V_{oc}, fill factor (FF) and EQE of 125 × 125 mm^2 cells are measured with calibrated 1-sun simulators.

3. Results and discussion

3.1. Observation results

Figure 1 shows the surface morphology of SiNWAs observed by scanning electron microscopy (SEM). The bright area in Fig. 1(a) is a loose Ag dendritic film on the SiNWA surface while the gray area is Si substrates before being cleaned well by HNO_3. Ag particles on the surface and at the bottom of the SiNWAs are shown in the inset of Fig. 1(a). SiNWAs with various lengths are prepared by changing the etch duration, and a sample of about 5 μm in length with a diameter of an individual NW ranging from 50 to 250 nm is shown in cross-sectional SEM in Fig. 1(b). The SiNWAs in sub-wavelength dimension of uniform length are fabricated on a large Si, as shown in the top view observation in Fig. 1(c). Etching of substrate B begins at the top of the pyramids and the pyramids would be mostly eaten away if the etching duration were long enough, as observed in Figs. 1(d) and 1(e). Controlling the etching time for an appropriate value would result in a hybrid textured structure composed of pyramid arrays and SiNWAs synthesized on substrate B, as shown in Fig. 1(f). The SiNWAs in the hybrid structure are grown on the sidewalls of the pyramid array and they are not vertical to the wafer but to the sidewall of pyramids certified by SEM observation, i.e. the Si is in [100] while the side wall of the pyramids is in [111]. Therefore, the preferential crystallographic orientation of the SiNWAs remains the same as on substrate A, although substrate B has the pyramid texture, which is consistent with the analysis of Chen *et al.*[13]. The etching rate at the bottom of the pyramids is lower than the top position, and the top of pyramids are almost eaten away completely when the etching duration is more than 3 h. According to the SEM observation of SiNWAs on polished wafers etched for different durations, one can generally conclude the relationship between the length of the SiNWAs versus etching time as depicted in Fig. 2. The linear fit relationship is also plotted in Fig. 2. Such nearly linear etching behavior facilitates the length control of SiNWAs on a large scale.

3.2. Reflection measurement

The as-synthesized samples seem extremely black, which reveals their possible excellent optical anti-reflectance ability. A 7-SCSpec solar cell spectral measurements system is used for reflectance (R) measurement of the NW arrays. The reflectance spectra of SiNWAs on a polished surface and a textured surface of varied etching times are shown in Figs. 3(a) and 3(b), respectively. The increasing etching duration decreases the reflectance of substrate A, and the reflectance is less than 3% in the wavelengths from 300 to 1000 nm when the

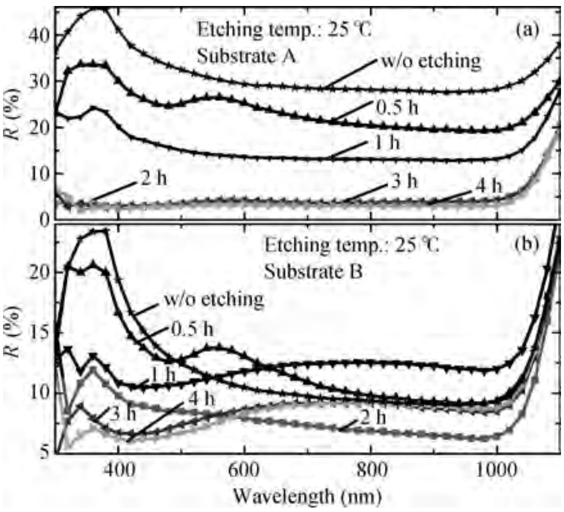

Fig. 3. Reflectance of substrates (a) A and (b) B etched for different times.

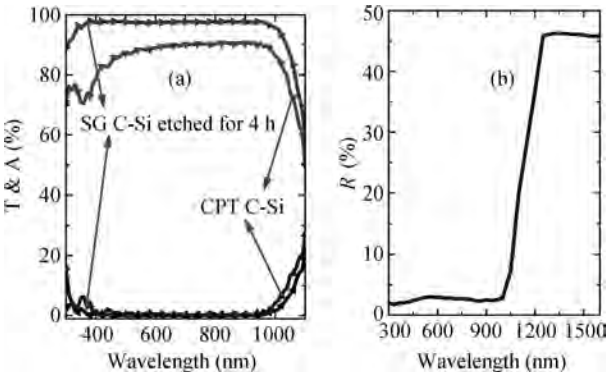

Fig. 4. (a) Transmission and absorptance of substrate A etched for 4 h and CPT C-Si. (b) Reflectance of C-Si NWs on substrate A in the wavelengths 300–1600 nm.

etching duration is longer than 2 h, as shown in Fig. 3(a). The reflectance of substrate A etched for 4 h is about 20% less than the CPT surface in the whole wavelength region and thus imparts a large reduction in reflectance. By the equation $R(\lambda) = 1 - A(\lambda) - T(\lambda)$, where λ is the optical wavelength, and R, T, A are the wavelength dependent reflectance, transmission, and absorption of the SiNWAs, respectively, the reduced reflectivity by a SiNW array can significantly increase the absorption ability. The absorption of substrate A etched for 4 h derived from transmission and reflectance is plotted in Fig. 4(a), in which the CPT C-Si is also plotted as a reference. As the figure shows, the absorption is larger than 95% and shows a more than 10% increase compared with CPT C-Si in the wavelength region of 400–1000 nm.

This observed reduction in the reflection for the etched samples can be explained by scattering theory. Compared to the diameter of the pyramids, which is of the order of μm, the diameter of Si NWs, e.g. from 50 to 300 nm, becomes comparable to the wavelength of the incident light. The incident light will be dominantly scattered according to sub-wavelength scattering theory and therefore prolongs the optical path length. Also, the SiNWAs introduce a possible porosity gradient, which also implies a change in refractive index with depth[10]. The above factors result in enhanced light absorption.

The reflectance of substrate B is more complex after the SiNWAs are fabricated, as shown in Fig. 3(b). The variations in diameter of the hybrid structure change the reflection properties in the whole wavelengths region. In short wavelengths, the wavelengths of the incident light are similar to the average diameter of Si NWs. Consequently, the scattering effect would be dominant, and thus significantly suppressed the transmission and decreased the reflection. However, in the long wavelengths, the SiNWAs would be much more appropriate for anti-reflection purposes, whereas the micrometer scaled pyramids deteriorate the anti-reflection properties. Therefore, there is a trade-off between the influence of both the pyramid array and the NW array on the reflection property for the long wavelength region. Accordingly, the reflection is firstly reduced and then enhanced in the reflectance spectra as the etching time increases. Simultaneously, we can conclude that the reflection reduction using the hybrid texturing structure is not prominent compared to that using the Si NW array only by Figs. 3(a) and 3(b). Thus the main mechanism of reflection reduction should be due to the involvement of Si NWs, which eventually enhances the absorption of SiNWA textured SCs.

For both substrates A and B, the reflectance increases sharply in the wavelength longer than 1000 nm, as shown in Fig. 4(b). According to the equation $\overline{R} = \frac{\int R(\lambda)\mathrm{d}\lambda}{\int \mathrm{d}\lambda}$, the average reflectance of substrate A is 2.52% in the wavelengths 300–1000 nm, where λ is the wavelength of the optical wave, and $R(\lambda)$ is the wavelength-dependent reflection coefficient. It is also noteworthy that the reflectance of our samples is comparable or much lower compared with those reported in the literature. For example, Peng *et al.*[10] obtained reflectance of 1.4% over the wavelength ranging from 300 to 600 nm for SiNWAs prepared on monocrystalline Si substrates. Rappich *et al.*[14] obtained reflectance values for nanoporous silicon ranging from $\sim$2%–30 % and $\sim$2%–20% in an anodized nanowire-like structure in the 300–850 nm wavelength range.

3.3. C-Si NW solar cells

SCs were fabricated on hybrid structure textured substrates without a SiN passivation layer (samples C1–C2) and with a SiN layer (samples D1–D2). SCs with SiNWAs were also manufactured on C-Si substrates where initial PN junctions were already formed (samples F1–F2) or not (samples E1–E3). We use a conventional silicon SC fabrication technique process including phosphorous diffusion to form a p–n junction, and screen-printing to form an aluminum back-surface-field and metal grid. Current–voltage curves of 125 × 125 mm^2 cells are measured under calibrated 1-sun simulators. Our best SiNWAs SC is made on C-Si substrate with an etching time of 2 h, and they have an efficiency of 12.45% with open-circuit voltage of 594 mV, short-circuit current of 34.82 mA/cm^2 and fill factor of 67%. Although the efficiency is not as high as commercial silicon solar cells, it is much better than the 9.31% SC with a $V_{\rm oc}$ of 548.5 mV reported by Peng *et al.*[15]. The best SC with a nanostructure as the anti-reflectance coating ever reported was made by Yuan *et al.*[16] with $V_{\rm oc}$, $J_{\rm sc}$, and FF of 612 mV, 34.1 mA/cm^2, and 80.6%, respectively. Compared

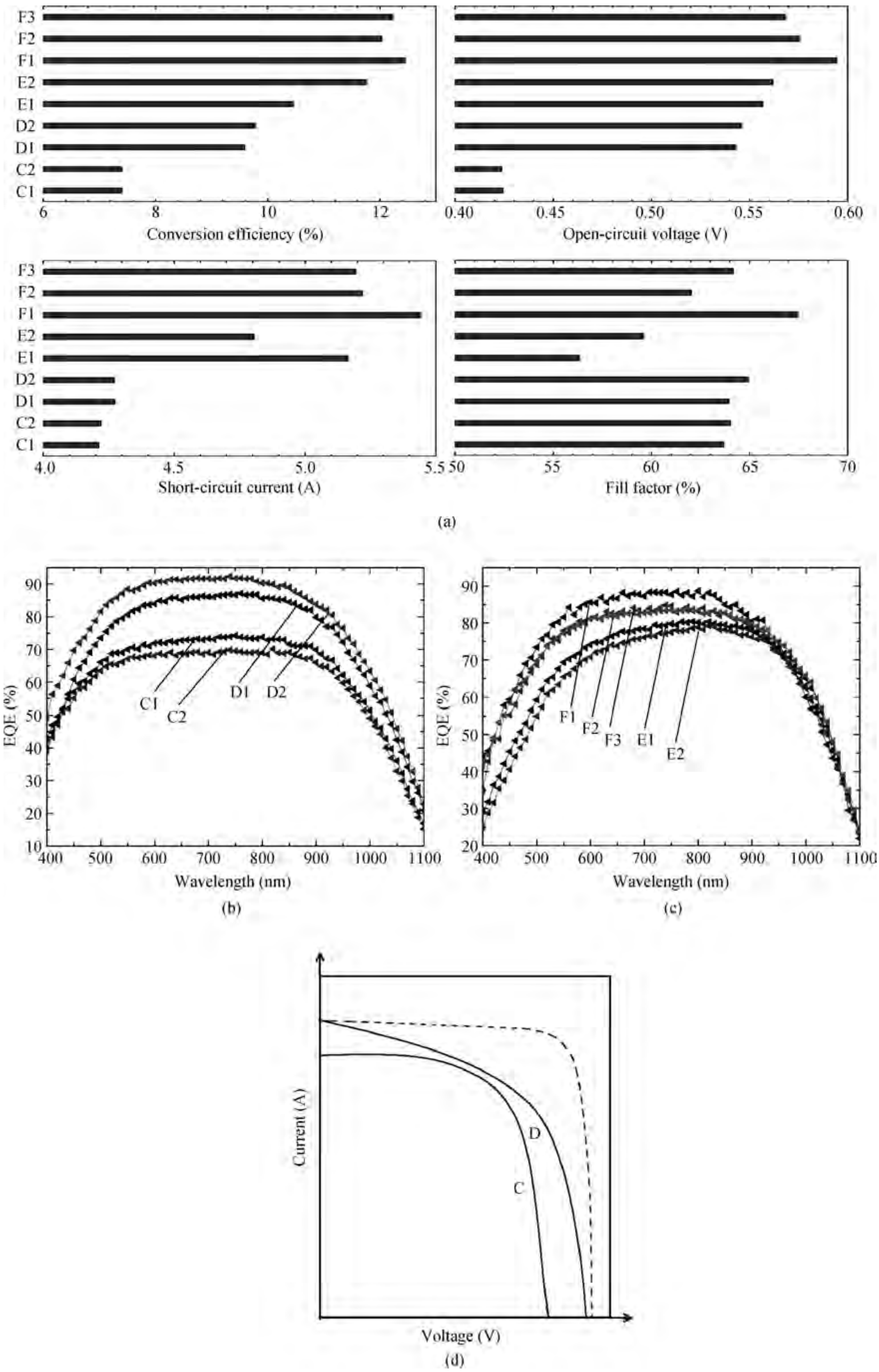

Fig. 5. Comparison of performance for different SC samples. (a) Comparison of conversion efficiency, V_{oc}, I_{sc} and FF. (b) EQE of samples C and D. (c) EQE of samples E and F. (d) Schematic diagram of low shunt resistance effect to sample D.

with their results, the I_{sc} of our best sample is improved by 0.71 mA/cm^2. Their as-grown thermal oxide passivation layer and as-evaporated metal grid matched their SC comparatively well and therefore their FF exhibits a better outcome than our sample and thus an optimized efficiency is obtained. Accordingly, if we fabricate a passivation layer and metal grid in a matched process, our sample may be optimized by improved V_{oc} and FF and thus conversion efficiency.

A comparison of basic parameters for different samples is plotted in Fig. 5. In order to investigate the ratio of absorbed photon energy to the converted electron energy, the EQE was measured as shown in Fig. 5. For our 7-SCSpec solar cell spectral measurements system, the measured area for EQE is about 2×2 cm^2. Based on the reflectance and absorptance analysis above, SiNWA SCs should correspondingly have high quantum efficiencies due to the excellent light-trapping characteristics of SiNWAs. Therefore, the EQE of SiNWA SCs should be enhanced prominently compared with CPT SCs. However, as shown in Fig. 5, the highest EQE of all samples is about 90%. The EQE degradation of NWs SC should be caused by high surface and interface recombination due to the high aspect ratio of SiNWAs. Thus, the electron–hole pairs cannot be collected effectively due to recombination. Generally, large V_{oc} reflects the relatively low surface recombination velocity of the Si/electrode junction and good bulk properties of NWs[15]. The average open circuit of 575 mV for our sample is relatively lower than the CPT cells, which is consistent with the poor passivation condition. Therefore, if perfect passivation is reached for the SiNWA SCs, the V_{oc} and correspondingly the conversion efficiency would be enhanced significantly. Comparing sample C with sample D, it is certified that the collection of photo-induced carriers could be improved by surface passivation, and therefore V_{oc} was enhanced prominently by 120 mV and correspondingly the efficiency was enlarged from 7.4% to 9.6% by nearly 30%. For the measured EQE of samples C and D, the short circuit current after passivation was also enlarged slightly (about 43 mA for 125×125 mm^2 cell), verifying the importance of a better passivation for cells with NWs. However, the I_{sc} enhancement of sample D is not very notable compared with V_{oc}, which may relate to the non-ideal I_{sc} measurement condition. For sample D, the shunt resistance is smaller than sample C for ten times (not shown). The smaller shunt resistance of sample D leads to the I–V curve dropping drastically, as depicted in Fig. 5(d). For a SC, an ideal I–V curve is like the dashed line in Fig. 5(d), and when the shunt resistance decreases, the I–V curve would change into line D[17]. Since the measured I_{sc} is a value under a voltage close to zero due to the outer series resistance, the measured I_{sc} of sample D is only improved by 0.06 A, which is not as large as the EQE.

Compared with sample E, both I_{sc} and V_{oc} of sample F are improved, but the most obviously improved parameter is the fill factor. The average FF of samples E and F is 57.9% and 64.5%, respectively. Therefore, if we made SiNWA SC on a substrate with a PN junction, the cell performance will be much better. Although the theoretical reason is still unclear, the main reason should be related to the metal grid contact characteristic based on the analysis of the FF data of samples E and F.

According to Fig. 5, we can conclude the general effects of imported SiNWAs to SCs. First, the fill factor is decreased compared with CPT SCs. This is attributed to high series resistance and reduced local shunting resistance. Thus the electrode fabrication process must be optimized for high efficiency SiNWA SC. Also, the FF shows a large vibration, which reflects that the stability is also a problem for SiNWAs. Second, the passivation affects the performance of SiNWA SC based on the result of samples C1–C2 and D1–D2. Accordingly, if a proper passivation layer is deposited on sample F, V_{oc} will be much higher and thus improve the cell efficiency. Finally, the performance of SiNWA SC can be improved by fabricating the SiNWA array on silicon substrates with PN junctions. This process improves the FF because the top of the SiNWA array which makes contact with the electrode is a highly doped area. To summarize, the performance of SiNWA SC can be optimized by the following two aspects. First, the fabrication process of the metal grid should be optimized in order to improve the FF. Second, the passivation layer suitable for SiNWAs must be developed to improve V_{oc} for high efficiency SiNWA SC. Therefore, systematic investigation of a matching fabrication process must be studied thoroughly in order to get a high performance SiNWA SC.

4. Conclusion

SiNWAs vertical to the Si, which exhibit strong anti-reflectance ability, as well as the hybrid structure of SiNWAs and pyramids, were fabricated by the aqueous chemical etching method. SiNWAs with different lengths can be realized by adjusting the etching duration or reaction temperature. Reflectance of the two kinds of structure—sole SiNWAs and hybrid structure of SiNWAs and pyramids—were measured and analyzed. The absorption of Si NWs is improved by more than 10% compared with CPT textured Si. The Si NW SCs were also fabricated and the EQE and basic parameters were measured. Our best SiNWA SC exhibits an efficiency of 12.45%, with open-circuit voltage of 594 mV, short-circuit current of 34.82 mA/cm^2 and fill factor of 60%. However, the recombination rates and surface state density are increased due to the high surface to volume ratio, which shrink the V_{oc} and correspondingly decrease the cell efficiency. Also, the FF of SCs with SiNWA structure is lower than CPT SCs. Therefore, the surface passivation and electrode fabrication on Si NWs are critically important when Si-NWs are employed in SC, and this should be studied thoroughly.

References

[1] Beyer T, Tacke M. Antireflection coating for PbSe diode lasers. Appl Phys Lett, 1998, 73: 1191

[2] Rajteri M, Rastello M L, Monticone E. Antireflecation coatings for superconducting photodetectors. Nucl Instrum Methods Phys Rev A, 2000, 444: 461

[3] Striemer C C, Fauchet P M. Dynamic etching of silicon for broadband antireflection applications. Appl Phys Lett, 2002, 81: 2980

[4] Green M A. Silicon solar cells: advanced principles and practice. Bridge, Sydney, 1995

[5] Kodambaka S, Tersoff J, Reuter M C, et al. Diameter-independent kinetics in the vapor-liquid-solid growth of Si nanowires. Phys Rev Lett, 2006, 96(9): 096105

[6] Morales A M, Lieber C M. A laser ablation method for the synthesis of crystalline semiconductor nanowires. Science, 1998,

279(5348): 208

[7] Wagner R S, Ellics W C. Vapor-liquid-solid mechanism of single crystal growth. Appl Phys Lett, 1964, 4(5): 89

[8] Greiner E S, Ellis W C, Gutowski J A. Preparation of silicon ribbons. J Appl Phys, 1961, 32(11): 2489

[9] Sandulova A V, Bogoyavlenskii P S, Dronyuk M I. Preparation and some properties of whisker and needle-shaped single crystals of germanium, silicon and their solid solutions. Sov Phys-Sol State, 1964, 5(9): 1883

[10] Peng K Q, Xu Y, Wu Y, et al. Aligned single-crystalline Si nanowire arrays for photovoltaic applications. Small, 2005, 1(11): 1062

[11] Hu L, Chen G. Analysis of optical absorption in silicon nanowire arrays for photovoltaic applications. Nano Lett, 2007, 7(11): 3249

[12] Min W L, Jiang B, Jiang P. Bioinspired self-cleaning antireflection coatings. Adv Mater, 2008, 20(20): 3914

[13] Chen C Y, Wu C S, Chou C J, et al. Morphological control of single-crystalline silicon nanowire arrays near room temperature. Adv Mater, 2008, 20(20): 3811

[14] Rappich J, Lust S, Sieber I, et al. Light trapping by formation of nanometer diameter wire-like structures on μc-Si thin films. J Non-Crystalline Solids, 2000, 266: 284

[15] Peng K Q, Wang X, Lee S T. Silicon nanowire array photoelectrochemical solar cells. Appl Phys Lett, 2008, 92(16): 163103

[16] Yuan H C, Yost V E, Page M R, et al. Efficient black silicon solar cell with a density-graded nanoporous surface: optical properties, performance limitations, and design rules. Appl Phys Lett, 2009, 95: 123501

[17] Green M A. Solar cells: operating principles, technology, and system applications. Englewood Cliffs, NJ, Prentice-Hall, Inc, 1982: 92